

## Measurement of diffusion and drift of charge carriers from photocurrent transients

Akiko Hirao and Hideyuki Nishizawa

*Materials and Devices Research Laboratory, Research and Development Center, Toshiba Corporation,  
1, Komukai Toshiba-cho, Saiwai-ku, Kawasaki 210, Japan*

(Received 18 March 1996)

A theoretical equation has been fitted to time-of-flight photocurrent transients of molecularly doped polymers in order to obtain the diffusion coefficient ( $D$ ) and drift mobility ( $\mu$ ) simultaneously.  $D$  and  $\mu$  did not show the sample thickness dependence such as was previously reported. The logarithm of  $D$  and  $\mu$  increased linearly with the square root of the electric field and decreased linearly with  $T^{-2}$ . The negative field dependence of the mobility in low electric field, obtained from the intersection time of asymptotes of the plateau and the trailing edge of the photocurrent transients, can be interpreted to be a result of the combination of drift and diffusion. [S0163-1829(96)03631-4]

### I. INTRODUCTION

Charge-transporting molecularly doped polymers (MDP's) constitute an amorphous system in which guest charge transport molecules are dispersed in the host polymer matrix. MDP's are systems in which the carriers are transported by hopping between zero-dimensional molecules, that is, single electron transfer systems. MDP's are widely used as transport layers for organic photoreceptors<sup>1-3</sup> and white-light-emitting organic electroluminescent devices.<sup>4</sup> Recent research on MDP's has revealed that they are potential materials for photorefractive devices,<sup>5,6</sup> for nonlinear optical fibers,<sup>7,8</sup> and for synapse bond devices.<sup>9</sup> The elementary process of any of these devices' operation involves carrier transport; hence carrier transport in MDP's has been the subject of numerous investigations.<sup>1-3,10-14</sup>

The standard method for characterizing carrier transport in MDP's is the time-of-flight (TOF) technique.<sup>1</sup> (See Fig. 1.) The time required for a packet of carriers generated by a pulse excitation to transit a sample of known thickness is measured. Typical photocurrent transients were observed to have an initial spike followed by a plateau, after which the current decayed as a function of time with a long tail.<sup>1</sup> This shape suggests that the packet of carriers spreads as it is transported because photocurrent transient has a rectangular shape in the case of nondispersive charge transport. The transit time, however, has usually been measured as the time at which the asymptotes of the plateau and trailing edge of the photocurrent transients intersect.<sup>15</sup> The transit time that is obtained by this method is not the average arrival time nor the arrival time of the first carrier. Therefore the physical meaning of the mobility obtained by this method is vague.<sup>16</sup> The mobility obtained from this transit time has, however, been examined<sup>1-3,17</sup> and in some cases it was seen to have thickness dependence.<sup>18-20</sup>

The diffusion coefficient, on the other hand, has not been discussed because it is difficult to measure. The diffusivity in ordinary crystalline semiconductors can be determined from mobility using Einstein's law relating carrier mobility to diffusivity.<sup>21</sup> Einstein's law, however, cannot be applied to

MDP's, which form nonequivalent and amorphous systems because the organic molecules in these systems essentially retain their identity, interacting only weakly through van der Waals forces, that is, the transfer integral is less than 0.01 eV.<sup>22,23</sup> Therefore, the diffusion coefficient of MDP's cannot be calculated using the mobility and needs to be measured separately.

The measurement of the diffusion coefficient is obviously necessary for practical purposes. The reason that the resolution of the image on the photoreceptor of the electrophotography is very low, being of the tens of micrometers, is thought to be due to the diffusion of carrier.<sup>24</sup> It is also thought to be due to diffusivity that anomalous broadening of the tails of TOF signals with electric field is observed.<sup>20</sup> Therefore, the measurement of carrier diffusion is thought to be very significant.

Many workers have reconsidered the interpretation of the shape of the TOF signals.<sup>25-28</sup> In the case of the analysis based on the multiple-trapping model, the photocurrent transients decrease continuously with time.<sup>26</sup> However, many workers have reported the photocurrent transients that have the plateau whose slope is zero or positive.<sup>29</sup> Analysis of a schematic TOF signal curve has shown that the effect of the diffusion is significant.<sup>1</sup> Assuming that the carrier packet is spread by diffusion and that each carrier drifts at a constant mobility in the sample, we examined the possible explanation for the shape of the photocurrent transients. An equation for the photocurrent transient in the case of the carrier-transported diffusing and drifting was fitted to the experimental TOF signal. We obtained a good fit between the theoretical equation and the experimental photocurrent transients. We thus finally succeeded in obtaining both diffusion coefficient and drift mobility from fitting.

In Sec. II, the TOF technique and fitting method of signals are described. The experimental photocurrent signal was fitted by the theoretical equation for the shape of photocurrent transients which is obtained by assuming that a carrier packet is spread by diffusion and that each carrier drifts in the sample at a constant mobility. Section III contains the results of fitting the theoretical equation to the experimental data

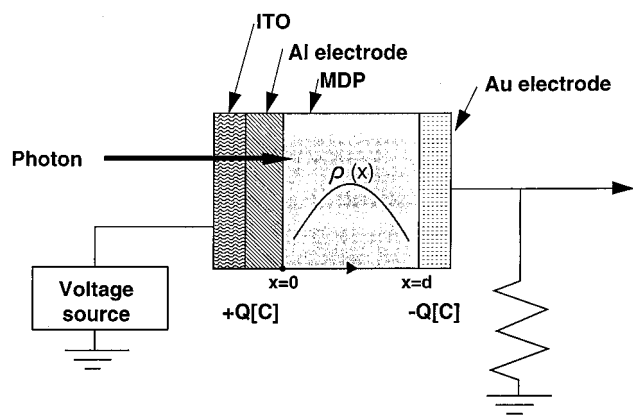


FIG. 1. A typical time-of-flight experimental arrangement for measuring hole mobilities.

and discussion. The sample thickness dependence of the mobility and the diffusion coefficient is analyzed along with the electric field and temperature dependence of the mobility. Then the empirical equation for the diffusion coefficient is presented. Using this empirical equation, the negative field dependence and thickness dependence of the mobility as obtained from the time at the intersection of the asymptotes of the plateau and the trailing edge of the photocurrent transients are explained. Finally the relationship between the drift mobility and the diffusion coefficient is presented.

## II. EXPERIMENTAL METHOD

### A. TOF measurement

Conventional TOF techniques<sup>1</sup> were used to obtain photocurrent transients over temperature ranges from 260 to 350 K and over electric field ranges from 1 to 36 MV/cm. Carrier transport in hydrazone-doped bisphenol-A-polycarbonate was analyzed. The doping concentration of *p*-diethyaminobenzaldehyde-diphenyl hydrazone (DEH) or 4-dibenzylamino-2-methylbenzaldehyde-1, 1-diphenylhydrazone (BMH) in the samples was 50% by weight. The measurements were made by conventional TOF techniques.<sup>1</sup> The molecular structural formulas for bisphenol-A-polycarbonate, DEH, and BMH are shown in Fig. 2. The MDP material was sandwiched between a semitransparent Al-coated quartz glass substrate and a Au electrode as shown in Fig. 1. From capacitance measurements, the thicknesses of the MDP's were determined. A sample with this sandwich structure was connected in a circuit with a voltage source and a resistance ( $R$ ). The MDP's were excited by a 0.9-ns nitrogen laser pulse (NDC, JS-1200) through the aluminum electrode. The penetration depths of the pulse into the MDP's were less than 0.1  $\mu\text{m}$ . These indicate that the penetration depths are small compared with the thicknesses of the MDP's. The energy per pulse incident on the MDP was adjusted such that the maximum charge generation in the MDP was less than  $0.03C_sV$ . Since the number of generated carriers is small enough, the local electric field caused by generated carriers is negligibly small in the measurement. The current transients were measured with a voltage amplifier (NF Electronic Instruments, BX-31A, DC~150 MHz) and a digitizing oscilloscope (Tektronix, model 11403, 10 bits, 1

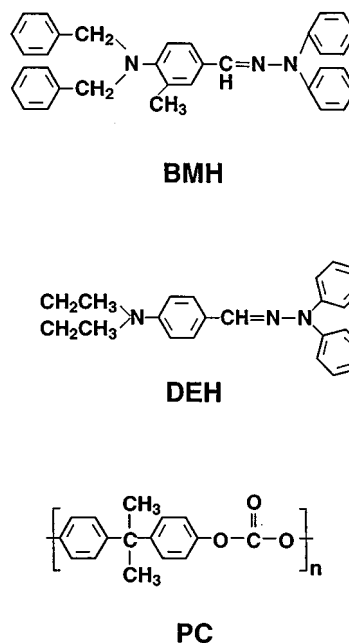


FIG. 2. Structural molecular formulas for (a) BMH, (b) DEH, and (c) bisphenol-A-polycarbonate.

GHz). Hence the digitizing noise will be small in the measurement. The sample holder was mounted in a temperature controlled chamber (Technolo, model CN-2). The time at the intersection of the asymptotes of the plateau and the trailing edge of the photocurrent transients was found to be 1000 times larger than  $C_sR$ . Over the range of fields and temperatures investigated, the transient shapes were reversible, with no signs of hysteresis.

### B. Parameter fitting of signals

The theoretical equation for the shape of photocurrent transients was derived assuming that a carrier packet is spread by diffusion and that each carrier drifts in the sample at a constant velocity.<sup>28,30</sup> Figure 3 is an illustration of this assumption. The photocurrent  $J$  is expressed by

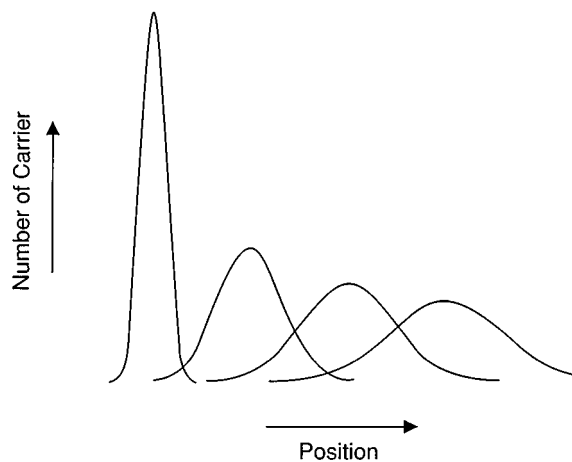


FIG. 3. An illustration of a transport of a carrier packet.

$$J = \frac{eD}{d} \frac{n_0}{\sqrt{4\pi Dt}} \left( \exp\left\{-\frac{(d-vt)^2}{4Dt}\right\} - \exp\left\{-\frac{(vt)^2}{4Dt}\right\} \right) - \frac{evn_0}{d} \frac{1}{2} \left( \operatorname{erf}\left\{\frac{vt}{\sqrt{4Dt}}\right\} + \operatorname{Flag} \operatorname{erf}\left\{\frac{|d-vt|}{\sqrt{4Dt}}\right\} \right),$$

$$\operatorname{Flag} = \begin{cases} 1, & d \geq vt \\ -1, & d \leq vt, \end{cases} \quad (1)$$

where  $v$  is the drift velocity,  $D$  is the diffusion coefficient,  $n_0$  is the number of holes ( $n_0 = q/e$ ),  $d$  is thickness of the sample, and  $\operatorname{erf}(x)$  is the error function.<sup>31</sup> The parameter fitting<sup>32</sup> of Eq. (1) to experimental signals that gives  $v$  and  $D$  was performed.

The parameter fitting method<sup>32</sup> is outlined below. The parameters of Eq. (1) to be fitted are  $D$ ,  $n_0$ , and  $v$ . First initial values of  $D$ ,  $n_0$ , and  $v$  and the permitted limits of fitting region  $\delta D$ ,  $\delta n_0$ , and  $\delta v$  were chosen. The second step, the calculation of variance between the observed data and the theoretical data, was obtained using Eq. (1) with the initial values. Next, random numbers,  $\beta_1$ ,  $\beta_2$ , and  $\beta_3$  lying between  $-1$  and  $1$  were generated using a computer. In the next step, the variance between the observed data and the theoretical data obtained using Eq. (1) with the values  $D + \delta D\beta_1$ ,  $n_0 + \delta n_0\beta_2$ , and  $v + \delta v\beta_3$ . If the variance became smaller than that obtained with the initial values, the initial value ( $D$ ,  $n_0$ , and  $v$ ) was replaced with  $D + \delta D\beta_1$ ,  $n_0 + \delta n_0\beta_2$ , and  $v + \delta v\beta_3$ , respectively. The above procedure was iterated until the most suitable values of the parameters were obtained.

### III. RESULTS AND DISCUSSION

#### A. Fitting of the equation to the signals

Figure 4 shows a typical photocurrent transient (solid line) that has a plateau and the fitting result (dotted line). We have succeeded in obtaining excellent fitting results for experimental data over temperature ranges from 260 to 330 K,

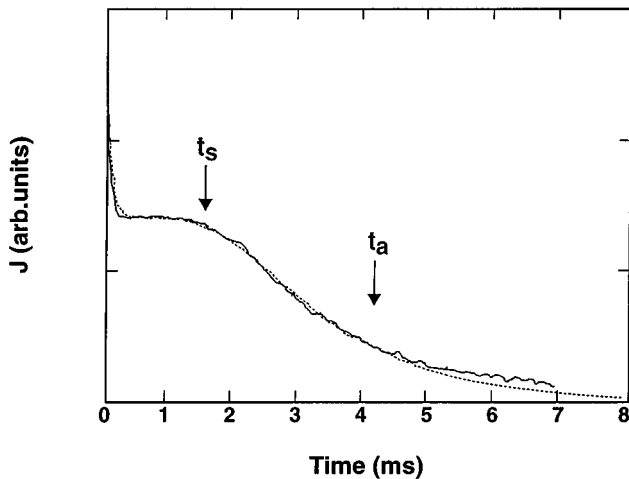


FIG. 4. A typical photocurrent transient that has a plateau. The solid line is the experimentally measured photocurrent and the dotted line is the current obtained by fitting the parameters of Eq. (1) to the experimental data.

and over electric field ranges from 1 to 36 MV/cm in our systems. We found that Eq. (1) was consistent with the experimental signal whose shape is nondispersive, except for the tail of the signal. In the region of the signal tail, experimental data were higher than the theoretical data. This difference could be attributed to two reasons. One is detrapping of the carrier from deep traps, because the density-of-states (DOS) profile is broad,<sup>1,10</sup> and carriers in the higher portion of the DOS profile could act as deep traps.<sup>12</sup> The other is a case where diffusion is anomalous.<sup>33</sup> For this case the mean-squared displacement is superlinear:

$$\langle r^2(t) \rangle \sim t^\gamma, \quad (2)$$

with  $\gamma \neq 1$ . If the hopping process is characterized within the framework of a random velocity walk,  $\gamma = 3/2$ . When  $\gamma > 1$ , the current value in the tail of the signal will become higher than the case of  $\gamma = 1$ . We will investigate this possibility in a future work.

The initial spike of the current is thought to correspond to motion of the holes at the illumination point ( $x \sim 0$ ). Since the motion of the holes at  $x = 0$  against the electric field does not exist, the holes at  $x = 0$  migrate by combining drift and forward diffusion. If the time constant of the external circuit of the experiment equipment is large, this initial spike in the current cannot be observed. If the penetration depth is not sufficiently small, the initial spike in the current will be small because the backward diffusion of holes also is observed as a current. In many cases, however, the initial spike has been observed. In addition to the above, the initial spike in the current has been simulated by Monte Carlo calculations.<sup>34</sup> Therefore the observed initial current spike can be fitted by Eq. (1). In this analysis, the initial spike can be understood to be produced by the spatial diffusion of carriers. On the other hand, Bäessler and co-workers developed the formalism that is based on fluctuations of site energies.<sup>10</sup> In their formalism, the initial spike can be understood to be due to the carrier thermalization within a disorder-induced DOS distribution. However, the current does not flow if the charge does not move. Hence it is a possible interpretation that the initial spike in the transient current is due to the carrier diffusion in the spatial description and the carrier thermalization in the energetic description simultaneously. We, therefore, conclude that the photocurrent transients in the MDP can be described by Eq. (1). Using the fitting procedure,  $D$ ,  $n_0$ , and  $v$  for each transient could be obtained.

The drift velocity ( $v$ ) obtained by the fitting allowed the transient time ( $t_a = v/d$ ) to be obtained. The time  $t_a$  was not equal to the time at the intersection of the asymptotes to the plateau and the trailing edge of the transient photocurrent ( $t_s$ ) as shown in Fig. 4. If the spread of the carrier packet that is described by the diffusion coefficient in this paper is zero,

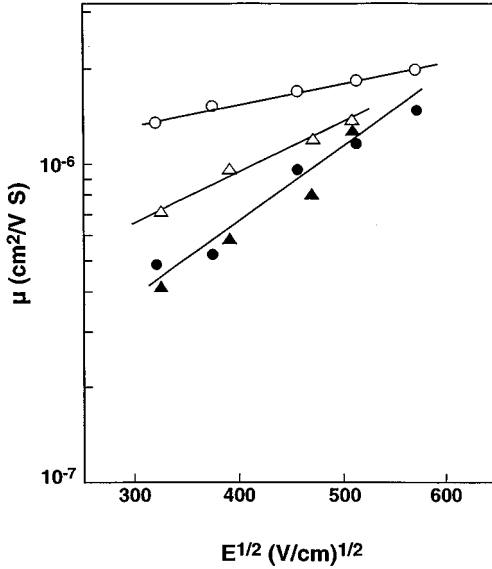


FIG. 5. Thickness dependence of logarithm of the mobility vs  $\sqrt{E}$  relationship for MDP of DEH at 300 K.  $\circ$ :  $\mu_s$  of 6.5  $\mu\text{m}$ ;  $\bullet$ :  $\mu_a$  of 6.5  $\mu\text{m}$ ;  $\triangle$ :  $\mu_s$  of 10.0  $\mu\text{m}$ ;  $\blacktriangle$ :  $\mu_a$  of 10.0  $\mu\text{m}$ .

$t_s$  is equal to  $t_a$ . Therefore the carrier diffusion leads to the difference between  $t_s$  and  $t_a$ . The time  $t_s$  is a time that is slightly larger than the arrival time of the earliest carriers at the collecting electrode.

### B. Dependence on sample thickness

In the past decade, most studies have described the mobility ( $\mu_s$ ) obtained from the time ( $t_s$ ) at the intersection of the asymptotes of the plateau and the trailing edge of the photocurrent transient. Many studies have focused on the thickness dependence of the mobility obtained by this technique.<sup>10-14</sup> Hence  $D$  and  $\mu_a$  which are calculated from  $t_a$  of samples of different thicknesses, have been measured by fitting. Figure 5 shows the electric field dependence of  $\mu_a$  at 300 K for 6.5- and 10.0- $\mu\text{m}$ -thick MDP of DEH. The logarithm of both mobilities can be seen to increase linearly with  $\sqrt{E}$ . The  $\mu_s$  that was obtained from the time ( $t_s$ ) at the intersection of the asymptotes of the plateau and trailing edge of the photocurrent transient for 6.5- $\mu\text{m}$  thickness was larger than the  $\mu_s$  for 10.0- $\mu\text{m}$  thickness. The electric field dependence of  $\mu_s$  was weaker when the sample thickness is smaller. However, the  $\mu_a$  values for the two samples obtained by the fitting procedure agree precisely as shown in Fig. 5. The  $D$  obtained simultaneously with  $\mu_a$  was also independent of thickness as shown in Fig. 6. These results imply that the  $\mu_a$  and  $D$  values obtained from the fitting are actual characteristic values of the substances in our systems. Therefore, the analysis of  $\mu_a$  and  $D$  from the fitting is physically meaningful.

### C. Electric field and temperature dependence of mobility

The electric field dependence of the mobilities calculated from  $t_s$  and  $t_a$  for MDP of BHM whose thickness was 5.4  $\mu\text{m}$  is shown in Figs. 7 and 8, respectively. The electric field dependence of  $\ln\mu_s$  calculated from  $t_s$  was similar to that of  $\ln\mu_a$ , except for negative field dependence in the low-

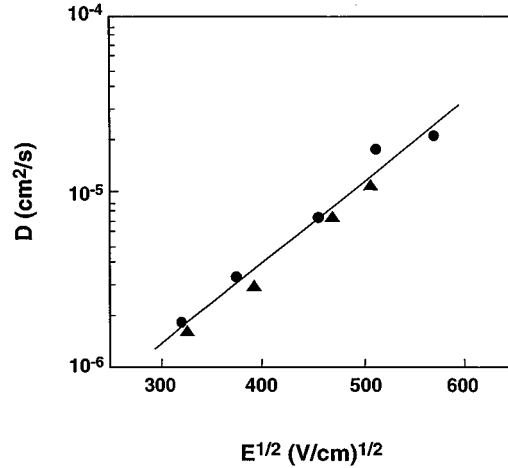


FIG. 6. Thickness dependence of diffusion coefficient vs  $\sqrt{E}$  for MDP of DEH at 300 K.  $\blacktriangle$ : 6.5  $\mu\text{m}$ ;  $\bullet$ : 10.0  $\mu\text{m}$ .

electric-field region. This negative field dependence of  $\mu$  in low electric fields has been reported by Borsenberger *et al.*<sup>35</sup> and Young and Pule.<sup>36</sup>

We analyzed  $\mu_a$  and  $\mu_s$  using the disorder formalism model.<sup>10</sup> In this approach,

$$\mu(T, E) = \mu_0 \exp\left[-\left(\frac{2\sigma}{3kT}\right)^2\right] \exp\left[C\left\{\left(\frac{\sigma}{kT}\right)^2 - \Sigma^2\right\}\sqrt{E}\right], \quad (3)$$

where  $\sigma$  is the width of the DOS profile,  $\Sigma$  is a parameter that describes the degree of the positional disorder,  $\mu_0$  is the mobility extrapolated to  $T \rightarrow \infty$  and  $E = 0$ , and  $C$  is an em-

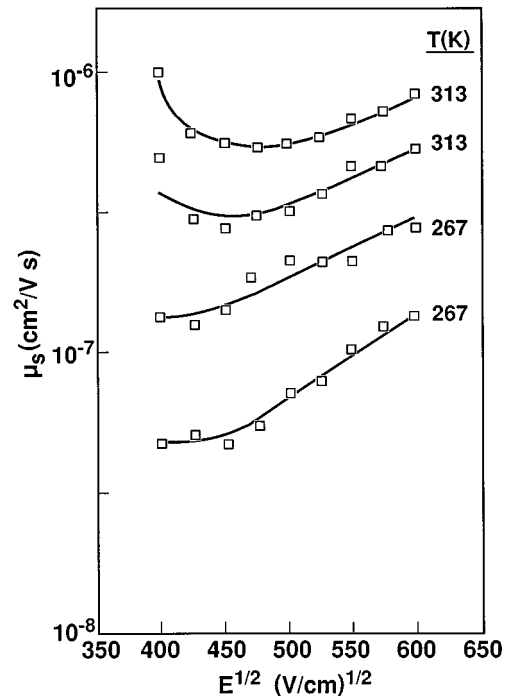


FIG. 7. Logarithm of the mobility  $\mu_s$  vs  $\sqrt{E}$  for MDP of BMH. The mobility  $\mu_s$  was obtained from the transit time defined as the time at which the asymptotes to the plateau and tail of the photocurrent profile intersect. Thickness of sample = 5.4  $\mu\text{m}$ .

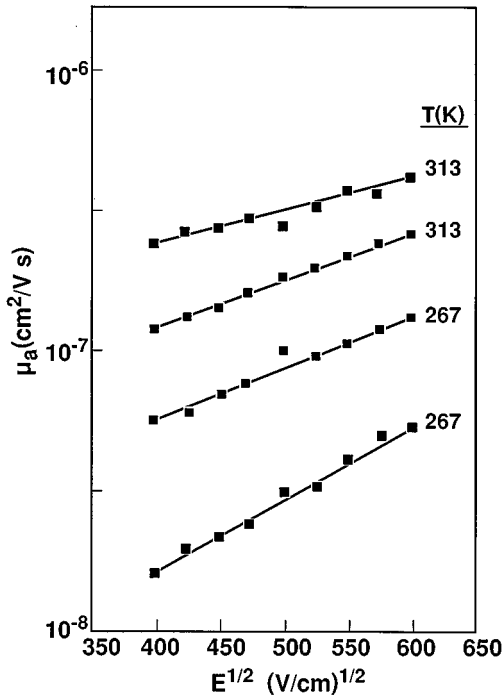


FIG. 8. Logarithm of the mobility  $\mu_a$  vs  $\sqrt{E}$  for MDP of BMH. The mobility  $\mu_a$  was obtained by fitting the parameters of Eq. (1) to the experimental signal. Thickness of sample = 5.4  $\mu\text{m}$ .

pirical constant. The results of this study showed that  $\mu_a$  could be described by Eq. (3). From the experimental results, the parameters of  $\mu_a$  were determined to be  $\mu_{a0} = 1.7 \times 10^{-2} \text{ cm}^2/\text{V s}$ ,  $\sigma_a = 0.14 \text{ eV}$ ,  $\Sigma_a = 4.2$ , and  $C_a = 2.9 \times 10^{-4} (\text{cm}/\text{V})^{1/2}$ .

Since the value of  $C_a$  is similar to the value of the disorder formalism,<sup>10</sup>  $\mu_a$  could be described using the disorder formalism model. Neglecting the negative field dependence at a low electric field, the parameters of  $\mu_s$  were determined to be  $\mu_{s0} = 9.2 \times 10^{-4} \text{ cm}^2/\text{V s}$ ,  $\sigma_s = 0.11 \text{ eV}$ ,  $\Sigma_s = 3.5$ , and  $C_a = 5.7 \times 10^{-4} (\text{cm}/\text{V})^{1/2}$ .

The  $\mu_s$  value was calculated using a time that was slightly larger than the arrival time of the earliest carriers at the collecting electrode. The earliest carriers are thought to be transported by a combination of drift and forward diffusion. Therefore, the negative field dependence of  $\mu_s$  in low electric fields could be attributed to the contribution of carrier diffusion in low electric fields. It is thought that the electric field dependence of  $\mu_a$  is much more pronounced than that of  $\mu_s$  because  $\mu_a$  does not contain a diffusion factor.

#### D. Electric field and temperature dependence of the diffusion coefficient

The logarithm of the diffusion coefficient for MDP of BMH increased linearly with the square root of the electric field in the same manner as MDP of DEH shown in Fig. 6. These are the first observations that the diffusion is assisted by the electric field in MDP systems. Field-assisted (biased) diffusion has been reported in simulation studies using the disorder model.<sup>23</sup> The temperature dependence of the diffusion coefficient can be seen in Fig. 9.

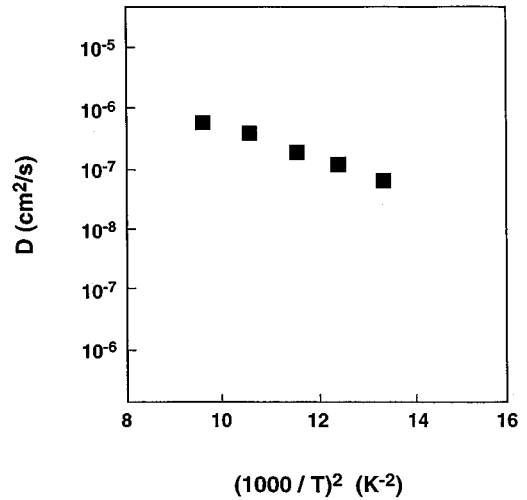


FIG. 9. Temperature dependence of the zero-field diffusion coefficient for MDP of BMH. Thickness of sample = 5.4  $\mu\text{m}$ .

We had analyzed the electric field and the temperature dependence of  $D$  using a deconvolution that was developed by Schein and co-workers.<sup>28,37</sup>  $D$  was represented by the following relationship:

$$D(T, E) = D_0 \exp\left[-\left(\frac{T_1}{T}\right)^2\right] \exp\left[C_d \left\{\left(\frac{T_1}{T}\right)^2 - \Delta\right\} \sqrt{E}\right], \quad (4)$$

where  $D_0$  is the diffusion coefficient extrapolated to  $T \rightarrow \infty$  and  $E = 0$ ,  $T_1$  is a constant, and  $C_d$  and  $\Delta$  are constants. The values of  $T_1$ ,  $D_0$ ,  $C_d$ , and  $\Delta$  were determined to be  $T_1 = 1150 \text{ K}$ ,  $D_0 = 3.3 \times 10^{-2} \text{ cm}^2/\text{s}$ ,  $C_d = 1.0 \times 10^{-3} (\text{cm}/\text{V})^{1/2}$ , and  $\Delta = 8.7$ . Equation (4) is similar to Eq. (3), which describes the drift mobility using the disorder formalism model.<sup>10</sup>

We can speculate on the interpretation of  $D$ , which depends on electric field. Increasing electric field affects the waiting time that originates the off-diagonal disorder for the carriers. Consider a case of hopping of a positive carrier on a site of which a neighbor hopping site does not exist in the forward direction of field on a microscopic scale. In this case, an overlap integral between the site and a forward hopping site is smaller than an overlap integral between the site and the neighbor hopping site. The positive carrier is transported forward by finding a path to new sites in which the overlap integral is larger in a low electric field without following the biasing field. In the case of higher electric field, however, due to a stronger force to the carrier from the biasing field, the probability of the carrier hopping to the neighbor site that is not situated in the forward direction of the field becomes lower (field enhanced trap). Therefore, the waiting time of the carrier becomes longer. In this system, increasing the biasing field affected the distribution of the waiting time and broadened the width of the carrier sheet. From this standpoint, the measurement of  $D$  may clarify a profile of off-diagonal disorder precisely.

Examples of physical manifestations of biased diffusion coefficient are the diffusion of particles in gels under gravity or subjected to centrifugal forces, as in chromatographic col-

umns and hopping electron conduction in doped semiconductors in the presence of strong electric fields.<sup>38</sup>

### E. Electric field and thickness dependence of $\mu_s$

In this section, we will present an explanation of the negative field dependence of  $\mu_s$ , at low electric fields seen in Fig. 7. The time  $t_s$  is slightly larger than the time of arrival of the earliest carriers that migrate by the combination of drift and forward diffusion. Therefore, the following relationship is obtained:

$$d = \mu_a E t_s + \alpha \sqrt{D t_s}, \quad (5)$$

where  $d$  is the sample thickness, and  $\alpha$  is a parameter. The term  $\alpha \sqrt{D t_s}$  is the distance between the center and the edge of the carrier packet. The mobility  $\mu_s$  is defined by

$$\mu_s = d / t_s E. \quad (6)$$

After substituting Eq. (5) into Eq. (6), we obtain

$$\mu_s = \mu_a / [1 - \{\sqrt{2P+1} - 1\}], \quad (7)$$

where  $P = \alpha^2 D / 2 \mu_a E d$ , and usually  $0 < P \ll 1$ . The  $S$  that represents the electric field slope of  $\mu_s$  is given by

$$\begin{aligned} \frac{\partial \ln \mu_s}{\partial \sqrt{E}} &= \frac{\partial \ln \mu_a}{\partial \sqrt{E}} + \frac{1}{1 - P(\sqrt{2P+1} - 1)} \\ &\times \left( \sqrt{2P+1} - 1 + \frac{1}{\sqrt{2P+1}} \right) \frac{\partial P}{\partial \sqrt{E}}. \end{aligned} \quad (8)$$

$\partial P / \partial \sqrt{E}$  can be described as

$$\frac{\partial P}{\partial \sqrt{E}} = \frac{\alpha^2 D}{2 d \mu_a E} \left( 2 \frac{\partial \ln \alpha}{\partial \sqrt{E}} + \frac{\partial \ln D}{\partial \sqrt{E}} - \frac{\partial \ln \mu_a}{\partial \sqrt{E}} - \frac{2}{\sqrt{E}} \right). \quad (9)$$

Since  $\sqrt{2P+1} - 1 > 0$ ,  $\partial \mu_s / \partial \sqrt{E} < 0$  requires  $\partial P / \partial \sqrt{E} < 0$ . After substituting Eqs. (3) and (4) into Eq. (9), we obtain

$$\begin{aligned} \frac{\partial P}{\partial \sqrt{E}} &= \frac{\alpha^2 D}{2 d \mu_a E} \left\{ 2 \frac{\partial \ln \alpha}{\partial \sqrt{E}} + \frac{1}{T^2} \left( C_d T_1^2 - \frac{\sigma^2}{k^2} \right) \right. \\ &\quad \left. - (C_d \Delta - C \Sigma^2) - \frac{2}{\sqrt{E}} \right\}. \end{aligned} \quad (10)$$

Using Eqs. (3), (4), (5), and (6), the values of  $\alpha$  of Eq. (5) can be calculated as shown in Fig. 10. From Fig. 10,  $\partial \alpha / \partial \sqrt{E}$  assumes negative. Therefore  $\partial P / \partial \sqrt{E}$  is negative at low  $E$ . Hence a negative field dependence of  $\mu_s$  at low electric fields is obtained by taking the contribution of carrier diffusion into account.

Equation (3) of the disorder formalism model indicates that the mobilities decrease with increasing field at low fields and high temperature. This is caused by the increase in the number of traps resulting from off-diagonal disorder (electric field induced traps).<sup>10</sup> However, the negative field dependence of  $\mu_s$  at low fields and low temperature cannot be explained by the disorder formalism model.

In Fig. 5, the thickness dependence of  $\mu_s$  was presented. Using Eqs. (3), (4), (5), and (6),  $\mu_s$  of samples of various thicknesses can be calculated. Figure 11 presents the electric

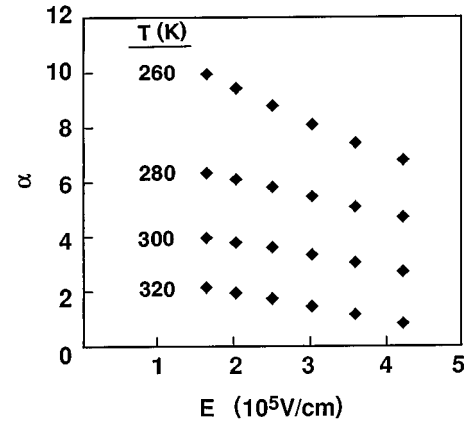


FIG. 10. Relationship between  $\alpha$  and electric field. Here, the parameters obtained for the MDP of BMH were used. Thickness of sample is  $5.4 \mu\text{m}$ . Here,  $T$  is the temperature.

field dependence of  $\ln \mu_s$  of the BMH's MDP over a thickness range from 2 to  $10 \mu\text{m}$  where  $\alpha = 1$  and  $T = 300 \text{ K}$ . The value of  $\alpha$  is dependent on the means of extrapolation. In order to clarify the tendency, we calculated  $\mu_s$  by assuming that  $\alpha$  is 1. The calculated results show the thickness dependence of  $\mu_s$  at low electric field. These results show a similar tendency to the experimental results of Fig. 5 of the Refs. 18 and 19. Therefore the thickness dependence of  $\mu_s$  at low electric fields seems to originate from the fact that  $\mu_s$  is calculated using a time near the time of arrival of the earliest carriers, which migrate by a combination of drift and forward diffusion.

### F. Relationship between $D$ and $\mu$

A combination of Eqs. (3) and (4) gives the relationship between  $D$  and  $\mu$ .  $\ln \mu_a$  is proportional to  $\ln D$  at a constant temperature and the slope of  $\ln \mu_a$  versus  $\ln D$  is greater than 1. Therefore, the increase of  $D$  with the electric field is much more than that of  $\mu_a$ . Richert, Pautmeier, and Bässler have reported that the results of their simulations indicate that diffusion coefficients increase with electric field much more

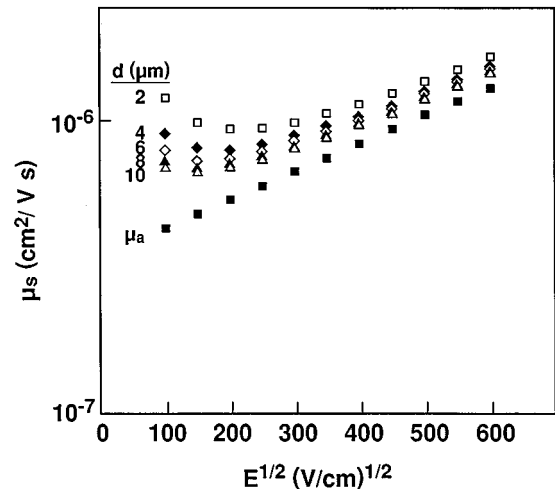


FIG. 11. Logarithm of  $\mu_s$  vs  $\sqrt{E}$ . Here,  $d$  is the sample thickness.  $\alpha = 1$ ,  $T = 300 \text{ K}$ .

rapidly than mobility.<sup>23</sup> Our experimental results matched their simulation results. It is natural that Einstein's law relating carrier mobility to diffusivity does not hold here.

#### IV. CONCLUSION

We have successfully fitted the theoretical equation to our experimental photocurrent transients whose shapes are non-dispersive over temperature ranges from 260 to 330 K, and over electric field ranges from 1 to 36 MV/cm. We obtained the drift mobility and the diffusion coefficient simultaneously by fitting. Since the mobility and the diffusion coef-

ficient were independent of the thickness of the samples, these seem to be actual characteristic values of the substance. The logarithm of the drift mobility increased linearly with the square root of the applied electric field. We found that the negative field dependence of the mobility obtained from the intersection time of the asymptotes of the plateau and trailing edge of the photocurrent transients at low electric fields appeared to be due to the combination of drift and forward diffusion. We also observed anomalous field-assisted diffusion first. The diffusion coefficients could be represented by the following relationship:  $D(T, E) = D_0 \exp[-(T_1/T)^2] \exp[C_d \{(T_1/T)^2 - \Delta\} \sqrt{E}]$ . These experimental results agreed with the simulation results.

- 
- <sup>1</sup>P. M. Borsenberger and D. S. Weiss, *Organic Photoreceptor for Imaging Systems* (Dekker, New York, 1993).
- <sup>2</sup>M. Scharfe, *Electrophotography Principles and Optimization* (Research Studies Press, Hertfordshire, England, 1983).
- <sup>3</sup>L. B. Schein, *Electrophotography and Development Physics*, 2nd ed. (Springer, New York, 1992).
- <sup>4</sup>J. Kido, K. Hongawa, K. Okuyama, and K. Nagai, *Appl. Phys. Lett.* **64**, 815 (1994).
- <sup>5</sup>S. Ducharme, J. C. Scott, R. J. Twieg, and W. E. Moerner, *Phys. Rev. Lett.* **66**, 1846 (1991).
- <sup>6</sup>W. E. Moerner and S. M. Silence, *Chem. Rev.* **94**, 127 (1994).
- <sup>7</sup>G. Kuzyk, U. C. Paek, and C. W. Dirk, *Appl. Phys. Lett.* **59**, 902 (1991).
- <sup>8</sup>K. P. B. Moosad, T. M. A. Rasheed, and V. P. Nampoor, *Opt. Eng.* **29**, 407 (1990).
- <sup>9</sup>H. Körner and G. Mahler, *Phys. Rev. B* **48**, 2335 (1993).
- <sup>10</sup>H. Bässler, *Phys. Status Solidi B* **175**, 15 (1993).
- <sup>11</sup>M. Sugiuchi and H. Nishizawa, *J. Image Sci. Tech.* **37**, 245 (1993).
- <sup>12</sup>H. Nishizawa, M. Sugiuchi, and T. Uehara, *Macromolecular Host-Guest Complexes: Optical, Optoelectronic and Photorefractive Properties and Applications*, MRS Symposia Proceedings Vol. 277 (Materials Research Society, Pittsburgh, 1992), pp. 33–38.
- <sup>13</sup>A. Hirao, H. Nishizawa, and M. Sugiuchi, *J. Appl. Phys.* **74**, 1083 (1993).
- <sup>14</sup>S. V. Novikov and A. V. Vannikov, *Chem. Phys. Lett.* **182**, 598 (1991).
- <sup>15</sup>R. C. Enck and G. Pfister, in *Photoconductivity and Related Phenomena*, edited by J. Mort and D. M. Pai (Elsevier, Amsterdam, 1976), Chap. 7.
- <sup>16</sup>L. Pautmeier, R. Richert, and H. Bässler, *Philos. Mag. B* **63**, 587 (1991).
- <sup>17</sup>A. Hirao, H. Nishizawa, and M. Hosoya, *Jpn. J. Appl. Phys.* **33**, 1944 (1994).
- <sup>18</sup>P. M. Borsenberger, L. T. Pautmeier, and H. Bässler, *Phys. Rev. B* **46**, 12 145 (1992).
- <sup>19</sup>H. Bässler and P. M. Borsenberger, *Chem. Phys.* **177**, 763 (1993).
- <sup>20</sup>H. J. Yuh and M. Stolka, *Philos. Mag. B* **58**, 539 (1988).
- <sup>21</sup>R. Kubo, M. Toda, and N. Hashitsume, *Statistical Physics II*, 2nd ed. (Springer-Verlag, Berlin, 1991), p. 178.
- <sup>22</sup>E. A. Silinsh, *Organic Molecular Crystals* (Springer-Verlag, Berlin, 1980), p. 36.
- <sup>23</sup>R. Richert, L. Pautmeier, and H. Bässler, *Phys. Rev. Lett.* **63**, 547 (1989).
- <sup>24</sup>E. J. Yarmchuk and G. E. Keefe, *J. Image Sci.* **35**, 231 (1991).
- <sup>25</sup>P. M. Borsenberger, L. T. Pautmeier, and H. Bässler, *Phys. Rev. B* **48**, 3066 (1993).
- <sup>26</sup>J. C. Scott, L. T. Pautmeier, and L. B. Schein, *Phys. Rev. B* **46**, 8603 (1992).
- <sup>27</sup>J. P. Bouchaud and A. Georges, *Phys. Rev. Lett.* **63**, 2692 (1989).
- <sup>28</sup>A. Hirao, H. Nishizawa, and M. Sugiuchi, *Phys. Rev. Lett.* **75**, 1787 (1995).
- <sup>29</sup>P. M. Borsenberger, L. Pautmeier, R. Richert, and H. Bässler, *J. Chem. Phys.* **94**, 8276 (1991).
- <sup>30</sup>S. M. Sze, *Physics of Semiconductor Devices* (Wiley, New York, 1981), p. 55.
- <sup>31</sup>*Handbook of Mathematical Functions*, edited by M. Abramovitz and I. A. Stegun (Dover, New York, 1970).
- <sup>32</sup>W. H. Press, B. P. Flannery, S. A. Teukolsky, and W. T. Vetterling, *Numerical Recipes in C* (Cambridge University Press, Cambridge, 1988), p. 548.
- <sup>33</sup>G. Zumofen, J. Klafter, and A. Blumen, *J. Stat. Phys.* **65**, 991 (1991).
- <sup>34</sup>P. Borsenberger, L. Pautmeier, and H. Bässler, *J. Chem. Phys.* **94**, 5447 (1991).
- <sup>35</sup>P. M. Borsenberger, E. H. Magin, M. van der Auweraer, and F. C. de Schryver, *Phys. Status Solidi A* **140**, 9 (1993).
- <sup>36</sup>R. H. Young and N. G. Pule, *Phys. Rev. Lett.* **72**, 388 (1994).
- <sup>37</sup>L. B. Schein, A. Rosenberg, and S. L. Rice, *J. Appl. Phys.* **60**, 4287 (1986).
- <sup>38</sup>S. Havlin, *Adv. Phys.* **36**, 695 (1987).